HHS Public Access

Author manuscript

Biochemistry. Author manuscript; available in PMC 2018 February 28.

Published in final edited form as:

Biochemistry. 2017 February 28; 56(8): 1130–1139. doi:10.1021/acs.biochem.6b01308.

Active Site Binding is not Sufficient for Reductive Deiodination by Iodotyrosine Deiodinase

Nattha Ingavat[†], **Jennifer M. Kavran**[‡,§], **Zuodong Sun**[†], and **Steven E. Rokita**[*,†]

[†]Department of Chemistry, Johns Hopkins University, 3400 North Charles Street, Baltimore, Maryland 21218 United States

[‡]Department of Biochemistry and Molecular Biology, Johns Hopkins Bloomberg School of Public Health, 615 North Wolfe Street Baltimore, Maryland 21205 United States

[§]Department of Biophysics and Biophysical Chemistry, Johns Hopkins School of Medicine, 925 North Wolfe Street Baltimore, Maryland, 21205 United States

Abstract

The minimal requirements for substrate recognition and turnover by iodotyrosine deiodinase were examined to learn the basis for its catalytic specificity. This enzyme is crucial for iodide homeostasis and the generation of thyroid hormone in chordates. 2-Iodophenol binds only very weakly to the human enzyme and is dehalogenated with a k_{cat}/K_m that is more than 4-orders of magnitude lower than that for iodotyrosine. This discrimination likely protects against a futile cycle of iodinating and deiodinating precursors of thyroid hormone biosynthesis. Surprisingly, a very similar catalytic selectivity was expressed by a bacterial homolog from *Haliscomenobacter hydrossis*. In this example, discrimination was not based on affinity since 4-cyano-2-iodophenol bound to the bacterial deiodinase with a K_d lower than that of iodotyrosine and yet was not detectably deiodinated. Other phenols including 2-iodophenol were deiodinated but only very inefficiently. Crystal structures of the bacterial enzyme with and without bound iodotyrosine are nearly superimposable and quite similar to the corresponding structures of the human enzyme. Likewise, the bacterial enzyme is activated for single electron transfer after binding to the substrate analog fluorotyrosine as previously observed with the human enzyme. A co-crystal structure of bacterial deiodinase and 2-iodophenol indicates that this ligand stacks on the active site FMN in a orientation analogous to that of bound iodotyrosine. However, 2-iodophenol association is not sufficient to activate the FMN chemistry required for catalysis, and thus the bacterial enzyme appears to share a similar specificity for halotyrosines even though their physiological roles are likely very different from those in humans.

[*]**Corresponding Author:** rokita@jhu.edu.

Supporting Information

The supporting information is available free of charge on the ACS Publications website at DOI: xxx. Protein purification, NMR data for 2IPCOOH, binding, kinetics, structural images and reduction of hhIYD (PDF)

Accession codes

The X-ray coordinates and structure factors have been deposited at the Protein Data Bank (PDB) under accession codes 5KO7, 5KO8 and 5KRD for hhIYD, hhIYD•I-Tyr and hhIYD•2IP structures, respectively.

Notes

The authors declare no competing financial interest.

TOC image

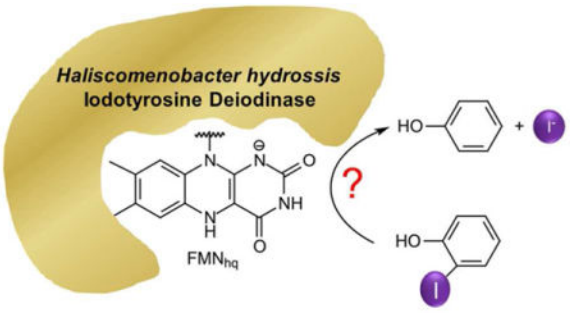

Iodotyrosine deiodinase (IYD) was first identified in nature by its ability to salvage iodide from iodotyrosine.[1] Iodide is an essential micronutrient for chordates if only for its iodination of thyroglobulin that serves as a precursor and template for generating the thyroid hormones thyroxine and triiodothyronine as well as their byproduct iodotyrosine (I-Tyr).[2] Chronic iodide deficiency is a result of a defective IYD,[3] and more generally, insufficient or excess iodide can cause severe disorders that affect human development and health.[4,5] Iodide generation by IYD also provides a rare example of reductive dehalogenation in aerobic organisms and is even more unusual for its dependence on flavin mononucleotide (FMN) (Scheme 1).[6] This enzyme also catalyzes dehalogenation of chloro- and bromotyrosine[7,8] but appears limited to processing simple tyrosine derivatives. Thyroxine (*O*-(4-hydroxy-3,5-diiodophenoxy)-3,5-diiodo-L-tyrosine) is also a tyrosine derivative but is not dehalogenated by IYD[9] and may not template a productive orientation of its active site residues.[10,11] Similarly, iodinated tyrosine residues on the surface of thyroglobulin are not predicted to serve as substrates for IYD due to their lack of a zwitterion for coordination with IYD.[10,11]

The selectivity of IYD for I-Tyr is essential to prevent a futile cycle of iodinating and deiodinating thyroxine and its precursors that could lead to thyroid disease. Sterics alone may exclude large compounds containing halogens from the active site of IYD but in the absence of substrate, its bound FMN is highly accessible[10,11] and sensitive to inhibition by many polycyclic haloaromatics such as triclosan, polychlorinated biphenyls and polybrominated diphenyl ethers.[12] If proximity to the reduced form of FMN (FMN_{hq}) were sufficient for dehalogenation than perhaps the halophenol component alone might act as a minimal recognition unit. In co-crystals of mammalian IYD and I-Tyr, the iodophenol component of I-Tyr stacks directly over the FMN and the aryl iodide bond is positioned above the region of FMN that is associated with electron and hydride transfer (C4a, N5). Aromatic stacking between substrates and FMN is not uncommon and was previously observed for nitroreductases that are in the same superfamily as IYD.[13,14] A similar substrate-FMN stacking was also evident for an azoreductase from *Pseudomonas*.[15] In addition, stacking between FMN and aromatic side chains of the surrounding protein is common and can dramatically influence the redox potential of FMN.[16]

Iodophenol and a few of its derivatives have now been examined with IYD to measure the intrinsic ability of this minimal unit to associate and react with the FMN. In addition, a potential correlation between ligand recognition and turnover has been examined as a basis

for substrate selection during reductive dehalogenation by IYD. Studies below reveal that binding of 2-iodophenol (2IP) to human IYD is very weak relative to that of I-Tyr. The origin of this specificity was subsequently challenged by using an alternative IYD from a bacterium, *Halisscomenobacter hydrossis*, for which the physiological substrate and metabolic role has not yet been defined. This IYD (hhIYD) demonstrated less stringency in substrate binding. X-ray crystal structures for hhIYD in the alternative presence of I-Tyr and 2IP are now described below and reveal that aromatic stacking between substrate and FMN is not sufficient to support efficient turnover.

MATERIALS AND METHODS

General Materials

Reagents of the highest grade available were used without purification. 3-Iodo-L-tyrosine (I-Tyr), 2-iodophenol (2IP), *m*-cresol and formic acid (88%) were obtained from Acros Organics. 3-Fluoro-L-tyrosine (F-Tyr) was purchased from Astatech, Inc. 4-Hydroxybenzoic acid was obtained from Alfa Aesar. 4-Cyano-2-iodophenol (2IPCN) was purchased from Pharmabridge, Inc. 4-Amino-2-iodophenol (4A2IP), xanthine and xanthine oxidase were obtained from Sigma-Aldrich.

4-Hydroxy-3-iodobenzoic Acid (2IPCOOH)

4-Hydroxybenzoic acid (830 mg, 6.0 mmol) was dissolved in conc. NH_4OH (aq) (29% w/w, 100 ml) and cooled to 4 °C while stirring. Iodine (1.5 g, 6.0 mmol) in EtOH (18 ml) was added dropwise to this solution over 1 h and the resulting mixture was stirred for another 2.5 h at 4 °C. The mixture was rotoevaporated to a reduced volume of 40 ml and then acidified to pH 2 by addition of HCl (1 N). The mixture was further rotoevaporated to dryness and the solid residue was dissolved in ethyl acetate (20 ml), washed twice with H_2O (20 ml) and rotoevaporated to dryness again. The crude product was dissolved in 20% aq. acetonitrile with 0.44% formic acid (v/v) and purified by reverse-phase HPLC (Econosphere C18 column; 250 × 10 μm) using a gradient of 20% to 30% acetonitrile in aqueous 0.44 % (v/v) formic acid over 15 min (5 ml/min). Fractions containing the product (t_R = 7 min) were lyophilized to yield 2IPCOOH as white solid (360 mg, 23 % yield). ^{1}H NMR (400 MHz, acetone-d_6) δ 7.05 (d, 1H, J = 8.4 Hz), 7.92 (dd, 1H, J = 2.0, 8.5 Hz), 8.40 (d, 1H, J = 2.0 Hz) (Figure S1); ^{13}C NMR (101 MHz, acetone-d_6) δ 82.9, 114.5, 123.8, 131.6, 141.2, 160.7, 165.4 (Figure S2). Both ^{1}H and ^{13}C NMR spectra are consistent with the literature.[17]

IYD Preparation

Human IYD without its N-terminal transmembrane sequence (residues 2–31) was expressed as a SUMO fusion as described previously.[11] IYD from *H. hydrossis* (hhIYD) does not contain a membrane binding sequence and was expressed as its full-length native sequence without a SUMO fusion. The hhIYD gene was amplified from a previous construct containing a SUMO fusion[18] using primers 5′-AATTAATCATATGAAGCAAAAGCCTGCTT-3′ and 5′-AATTAATCTCGAGCTAGTGATGGTGATG-3′. This provided a 5′-flanking NdeI site and a 3′-flanking XhoI site that were used to subclone the gene into a pET-24a(+) vector. The resulting hhIYD gene contained a C-terminal His_6 tag. Both human IYD and hhIYD were

expressed and purified (Ni^{2+} affinity and size exclusion chromatography) as described previously.[11,18] Only the induction conditions for both IYDs were modified by lowering the isopropyl β-D-1-thiogalactopyranoside concentration from 400 μM to 20 μM, decreasing the induction temperature from 18 °C to 16 °C and increasing the induction time from 4 h to 12–16 h.

General Methods

Protein concentrations for crystallization studies were determined by A_{280} (ε_{280} = 37,930 M^{-1} cm^{-1} for human IYD and ε_{280} = 31,400 M^{-1} cm^{-1} for hhIYD as estimated by ExPASy ProtParam tool)[19] after correcting for the contribution of its bound FMN (A_{280}/A_{450}, 1.9 ± 0.1 for human IYD and 1.72 ± 0.04 for hhIYD). Enzyme concentrations for kinetic and binding studies were determined by A_{450} derived from the bound FMN (ε_{450}, 13,000 ± 300 M^{-1} cm^{-1} for human IYD and 13,600 ± 300 M^{-1} cm^{-1} for hhIYD) as determined from the native enzyme and free FMN (ε_{450} = 12,500 M^{-1} cm^{-1})[20] released after heat denaturation and removal of the protein by centrifugation and Ni^{2+} affinity chromatography. Dissociation constants (K_d) for the ligands of IYD were determined by their ability to quench the fluorescence of the oxidized FMN (FMN_{ox}) (λ_{ex} 450, λ_{em} 523 nm) in the active site of IYD as previously described.[11,21]

Catalytic Deiodination

Catalytic turnover of IYD was observed by quantifying the product of deiodination after separation by reverse-phase HPLC as previously described.[22] Briefly, iodinated substrates were incubated with hhIYD in 100 mM potassium phosphate pH 7.4 and reaction was initiated by addition of 0.5% dithionite in 5% sodium bicarbonate. This mixture was incubated at 25 °C for the specified time and then quenched with 88% formic acid. Internal standards of either *m*-cresol or benzoic acid were used to quantify formation of each product. See Figure S5–S7 for more details. Studies with human IYD followed the same procedures but contained an additional 200 mM KCl to stabilize the enzyme.

Anaerobic reduction of hhIYD by xanthine and xanthine oxidase

Solutions of hhIYD (20 μM), potassium phosphate (100 mM, pH 7.4), sodium chloride (500 mM), glycerol (10% v/v), xanthine (1 mM) and methyl viologen (13 μM) were purged of molecular oxygen by gently bubbling with Ar for 30 min. Reduction was initiated by addition of xanthine oxidase (140 μg/mL) as previously described.[11,23,24] Enzyme reduction was repeated in the alternative presence of F-Tyr (500 μM) and 2IP (800 μM) to study the effect of ligand on the redox properties of hhIYD.

Crystallization

Crystallization conditions were determined using sparse matrix screening with commercially available screens and a Phoenix robot. Crystals of hhIYD without ligand were grown by mixing 1 μl of protein (13 mg/ml, in 50 mM sodium phosphate pH 7.4, 100 mM NaCl, 0.5 mM TCEP and 10 % glycerol) with 0.8 μl of well solution containing 80 mM Tris-HCl pH 8.5, 100 mM $MgCl_2$, 24% (w/v) PEG 4000 and 20% glycerol. To obtain co-crystals of hhIYD and I-Tyr, hhIYD 13 mg/ml (final), in 25 mM HEPES pH 7.4, 0.5 mM TCEP and

10 % glycerol was incubated with 2 mM (final) of I-Tyr overnight at 4 °C. Crystals were grown by mixing 0.8 μl of hhIYD•I-Tyr with 1 μl of well solution containing 100 mM HEPES pH 7.5, 150 mM $MgCl_2$, 25% (w/v) PEG 3350, 2 mM I-Tyr and 15% glycerol. To obtain a complex of hhIYD with 2IP, hhIYD (15 mg/ml, final) in 25 mM HEPES pH 7.4, 0.5 mM TCEP and 10 % glycerol was incubated with 2 mM (final) of 2IP overnight at 4 °C. Crystals were grown by mixing 1 μl of hhIYD•2IP with 0.8 μl of well solution containing 100 mM Tris-HCl pH 9, 200 mM $MgCl_2$, 2 mM 2IP, 17% (w/v) PEG 8000, 17% glycerol and 10% (v/v) ethylene glycol. Crystals were grown at 20 °C by hanging drop vapor diffusion and appeared within 3 days. Crystals were frozen in liquid nitrogen directly from the mother liquor prior to data collection.

Data Collection and Structure Determination

Diffraction data were collected at the 12-1 and 7-1 beamlines at the Stanford Synchrotron Radiation Lightsource (SSRL) and processed with either XDS/Aimless[25] (for PDB 5KO7 and 5KO8) or HKL2000/Scalepack[26] (for PDB 5KRD). Phases were determined by molecular replacement with PHASER[27] using the mouse IYD structure (PDB 3GB5) as the search model.[10] All three structures were built and refined by iterative rounds of model-building in COOT[28] and refinement in PHENIX.[29] All structural figures were drawn with PyMOL (Schrödinger, LLC).

RESULTS

Expression and Purification of IYD

Expression of mammalian IYD had been problematic until development of a His_6-tagged SUMO-fusion.[11,30] This construct reproducibly provides soluble and active enzyme in good yield from *Escherichia coli*. SUMO fusions were hence used when testing the activity of IYD homologs from other organism including *H. hydrossis*.[18] In this and other examples, purification was often complicated by co-elution of IYD and the hydrolyzed SUMO. In attempt to optimize IYD purity for crystallization trials, the native sequence of hhIYD was expressed without a SUMO fusion. Previously, IYD from *Drosophila melanogaster* was successfully prepared under these conditions,[22] and hhIYD provided similar success. Human IYD from the IYD-SUMO fusion and native hhIYD lacking an attached SUMO were both isolated in yields of 15–24 mg/L of culture with purity of > 98% as evident from SDS-PAGE, coomassie staining and ImageQuantTL analysis (Figure S3). The size of the IYD polypeptides indicated by denaturing gel electrophoresis (30 kDa and 25 kDa for human IYD and hhIYD, respectively) are consistent with the estimates generated by ExPASy.[31] Native IYD exists in solution as a homodimer and preparations contained ratios of 1.9 – 2.1 FMN per dimer as measured by A_{450} and A_{280}. This ratio indicates approximately full loading of the cofactor based on the theoretical maximum of 2.0.[18]

Substrate and Ligand Binding to IYD

Binding of tyrosine and phenol derivatives to the active site of IYD can be monitored by their ability to quench the fluorescence of its FMN_{ox}.[7] To assess the contribution of the aromatic component of I-Tyr on binding, affinities of I-Tyr and 2IP were initially compared using human IYD. Previously, the K_d of I-Tyr was observed in the sub-μM range and a

similar value of 0.09 μM was measured in this study (Figure 1, Table 1). In contrast, 2IP expressed only a weak affinity for human IYD as evident by an increase in K_d by more than 4-orders of magnitude. Thus, the human enzyme requires the zwitterion of I-Tyr for tight binding and is likely limited to substrates containing such a zwitterion in vivo. This selectivity is also essential for proper thyroid function.

The necessity of a similar selectivity in lower organisms and particularly bacteria is not apparent since the generation and function of halotyrosines in these organisms have not yet been established.[32,33] The role of the aromatic component of I-Tyr in the absence of its zwitterion was therefore interrogated with hhIYD as well. Using the same fluoresence assay, I-Tyr was found to bind hhIYD with a ~90-fold weaker affinity than human IYD (Figure 1, Table 1). In contrast, 2IP exhibited a ~20-fold increase in affinity for hhIYD relative to human IYD. Thus, the halophenol component contributes more to the binding of I-Tyr with hhIYD than with human IYD. This difference had the potential to suggest a broader substrate profile for hhIYD versus human IYD.

The promiscuity of halophenol binding to hhIYD was further challenged by three additional derivatives alternatively adding a charge (4-hydroxy-3-iodobenzoate, 2IPCOOH), an electron withdrawing group (4-cyano-2-iodophenol, 2IPCN) or an electron donating group (4-amino-2-iodophenol, 4A2IP) to the parent iodophenol. Previous studies with human IYD demonstrated preferential binding to the phenolate form of diiodotyrosine (I_2-Tyr)[11] and hence the shift in acidity caused by the cyano and amino substituents were used to test if a similar preference would also extend to the binding of simple phenols to hhIYD. The calculated pK_a for 4A2IP is only slightly higher than that for 2IP but, as anticipated, the K_d value observed for 4A2IP is 40% larger than that for 2IP (Table 1). However, this difference may not be significant since much of the fluorescence quenching data of 2IP and 4A2IP are experimentally indistinguishable (Figure S4). Differences in the pK_a and K_d values of 2IP and 2IPCN are considerably more pronounced. The acidity of 2IPCN is greater by 2 pK_a units than that of 2IP and the K_d value of 2IPCN is almost 50-fold lower than that of 2IP (Table 1 and Figure S4). 2IPCN affinity for hhIYD is even greater than that of I-Tyr. This could imply that zwitterion recognition may not be crucial for hhIYD catalysis but results below highlight differences in the criteria for binding and turnover. Both the acidity of 2IPCOOH and its affinity for hhIYD are intermediate between 2IP and 2IPCN (Table 1), and the presence of an additional negative charge of the carboxylate does not significantly affect recognition by the active site of hhIYD.

Catalytic Deiodination

Enzyme turnover of each potential substrate was monitored by formation of its deiodinated product after separation by reverse-phase HPLC (Figures S5 and S6) and the kinetic constants were determined by measuring initial rates as a function of substrate concentration (Figure S7). As typical for IYD, dithionite was used as the reductant since the physiological system for reduction has yet to be identified.[34] The k_{cat} value for deiodination of I-Tyr by human IYD (Table 1) is nearly identical to that recently determined for *Drosophila* IYD (12 × 10^{-2} s^{-1})[22] and in both examples their K_m values are more than 20-fold (*Drosophila*) and 80-fold (human) greater than their K_d values. The steady-state parameter k_{cat}/K_m for

turnover of I-Tyr by human IYD is also within two-fold of its second order k_{ox} for I-Tyr dependent oxidation of FMN_{hq} as measured by rapid kinetics.[8] Similarly, the k_{cat}/K_m value for I-Tyr is only 50% larger than that measured for I_2-Tyr using a complementary ^{125}I-iodide release assay.[11] The lack of the zwitterion in 2IP greatly compromises its turnover by human IYD. The k_{cat} for 2IP is 26-fold less than that for I-Tyr and, even more significantly, the K_m for 2IP is 560-fold greater than that for I-Tyr (Table 1). This large increase in K_m is still less than the 16000-fold increase in the K_d for 2IP versus I-Tyr (Table 1).

Despite the lower affinity of I-Tyr for hhIYD relative to human IYD, hhIYD expresses a higher catalytic efficiency as indicated by the 16-fold increase in its k_{cat}/K_m value (Table 1). Deiodination of I-Tyr is also more efficient than that of I_2-Tyr for hhIYD as well as for human IYD.[11,18] The loss in efficiency for deiodination of 2IP lacking the zwitterion of I-Tyr is even more dramatic for hhIYD. The decrease in k_{cat}/K_m from I-Tyr to 2IP is 33,000-fold and twice as large as that for human IYD. The physiological substrate for hhIYD has not yet been identified, but clearly this enzyme is not a general dehalogenase for halophenols. The low rates of 2IP turnover by both IYDs are still faster than the intrinsic reactivity between the free cofactor FMN_{hq} and 2IP. Under standard conditions in the presence of FMN (2.5 μM), 2IP (5 mM) and dithionite (0.5% w/v), no phenol was detected above the threshold of ~ 3 nmol after a 2 h incubation (Figure S8). However, the enhanced binding of 2IP to hhIYD versus human IYD did not result in a significant gain of catalytic efficiency.

Turnover of the 2IP derivatives was also investigated to learn whether the active site affinity of these minimal structures might still influence catalysis. Kinetics were again monitored by formation of the deiodinated products after separation by reverse-phase HPLC (Figures S5 – S7). 2IPCOOH exhibited a k_{cat} that was experimentally indistinguishable from that of 2IP and the k_{cat}/K_m values for both compounds were both quite minimal (Table 1). However, the K_m for 2IPCOOH was 75% larger than that for 2IP and contrary to the hierarchy of their K_d values. The activity of 4A2IP was also not consistent with its relative binding affinity for hhIYD since its k_{cat}/K_m value was almost 6-fold greater than the parent 2IP (Table 1). Poor solubility of 4A2IP restricted its further characterization. Likewise, the lack of detectable product provided only a lower estimate for turnover of 2IPCN. Speculation on the electronic demands of dehalogenation from the data on 4A2IP and 2IPCN is tempting but should be deferred until a comprehensive structure-activity survey can be completed. Still, the inability for IYD to deiodinate 2IPCN was initially surprising since 2IPCN binds the resting enzyme even more tightly than I-Tyr (Table 1).

Crystallographic Studies of hhIYD

The structures of hhIYD in the absence of substrate and bound to either I-Tyr or 2IP were compared to their mammalian counterparts to examine the structural basis for a lack of correlation between halophenol binding and catalysis. Crystals of hhIYD, hhIYD•I-Tyr and hhIYD•2IP diffracted X-rays to 2.3 Å, 2.2 Å, and 2.1 Å, respectively, and the phases of each were determined by molecular replacement using the mouse IYD structure as a search model (Figure 2).[10] Data collection and refinement statistics are summarized in Table 2. Unbiased electron-density indicated the position of substrates, and the signal from anomalous

difference maps was used to place the iodine atom of each ligand (Figure 3). Like its mammalian homologs, the biological active form of hhIYD is an α_2 dimer. The asymmetric unit contains the biological dimer for hhIYD in the absence of ligand. The biological dimers are not contained within the asymmetric unit for hhIYD in the presence of ligand (hhIYD•I-Tyr and hhIYD•2IP) and were instead generated by crystal symmetry. In each case the two subunits of each α_2 dimer are nearly identical and only one chain will be discussed unless otherwise indicated.

Structure of hhIYD

The structure of hhIYD in the absence of substrate displays the common features of the nitro-FMN reductase superfamily for which IYD is a member.[35] Despite sharing only 44% sequence identity, human IYD and bacterial hhIYD have the same fold and superpose with an RMSD of 0.77 Å for 321 Cα atoms (Figure S9A). The two subunits of hhIYD form a dimer containing an α-β fold with domain swaps at the N- and C-termini. Each dimer has two active sites that are formed by regions of each monomer, and each contain a FMN bound noncovalently (Figure 2A). In the absence of substrates, the structures of IYD from *H. hydrossis*, human, and mouse have a disordered active site lid (Figure S9). In hhIYD, the loop adjacent to the active site (residues 133–145) is ordered in the absence of substrate whereas in human IYD, this loop is only ordered upon I-Tyr binding.[11] Substrate binding is not even sufficient for fully ordering this loop in mouse IYD.[10] The enhanced stability of this loop in hhIYD may be rationalized by the rigidity introduced by substitution of an Ala in human and mouse IYD for a Pro137 in hhIYD (Figure S10).[36] Additionally, Asp138 and Thr140 are within hydrogen bonding distances in hhIYD but are substituted with Gln and Lys in human and mouse IYD, respectively.[10,11]

Structure of hhIYD•I-Tyr

Comparison of the structures of hhIYD in the presence and absence of I-Tyr revealed no large scale conformational changes (RMSD of 0.23 Å for 345 Cα atoms) upon ligand binding except for an ordering of the active site lid (residues 95–112) (Figure 2B). Similar conformational changes were observed in the structures of both mouse and human IYD bound with substrates.[10,11] In each case, the active site lid is stabilized by interactions between the zwitterion of I-Tyr and a common set of residues that are illustrated by Glu91, Tyr95 and Lys116 in hhIYD (Figure 2E). These residues are evident in all IYD homologs confirmed to date and have been used to detect other likely deiodinases within the parent nitro-FMN reductase superfamily.[18] The zwitterion of I-Tyr also offers hydrogen bonding through its α-ammonium group to the FMN O^4 and through its carboxylate group to the FMN N3. Other features that stabilize the substrate-enzyme complex include hydrogen bonding between the phenolate of I-Tyr and the amide backbone of Ala 64 and 2′-HO-ribityl of FMN and π-stacking between the aromatic region of I-Tyr and the isoalloxazine ring of FMN (Figure 2E). These interactions are also evident in substrate complexes formed by mouse and human IYD.[10,11]

For hhIYD•I-Tyr, the active site lid could be fully built for one active site but only partially built for the other suggesting that the lid is not in a single fixed orientation when bound to I-Tyr. The electron density maps also revealed that I-Tyr aligns in two orientations with

respect to the iodo substituent instead of the single orientation observed in the mammalian IYD structures.[10,11] Greater density is evident for an alignment of the aryl-I bond over the C4a-N5 bond of FMN and consistent with that for mammalian IYD (Figure 3A).[10,11] The alternative conformation represents a ~ 180° flip of the aryl ring. In this orientation, the aryl-I bond resides above the pyrimidine ring of FMN and toward Phe110 (3.3 Å). Phe110 likely stabilizes this alternative conformation by offering favorable C−I···π interactions that are not available in the mammalian structures.[37]

Structure of hhIYD•2IP

The structure of hhIYD bound with 2IP is similar to that bound with I-Tyr but lacks an ordered active site lid. hhIYD•2IP also superposes with hhIYD lacking an active site ligand with an RMSD of 0.30 Å for 337 Cα atoms (Figure S9D). Analysis of unbiased difference maps for hhIYD bound with 2IP reveal electron-density for only the iodo group and phenolate oxygen suggesting that the ring of 2IP is mobile (Figure 3B). The orientation of 2IP aligns the aryl-I bond over the C4a-N5 of FMN as observed previously for I-Tyr bound to the mammalian IYDs. By extrapolation from these structures, 2IP likely interacts with hhIYD through π-stacking with the isoalloxazine ring of FMN and hydrogen bonding between the phenolate of 2IP and the amide backbone of Ala64 and the 2′-HO-ribityl of FMN (Figure 2F). The distance between the iodo substituent and N5 of FMN is relatively constant at ~ 4 Å for the structures containing either I-Tyr or 2IP (Figures 2E and 2F). In contrast to I-Tyr, no zwitterion is provided by 2IP to coordinate the FMN and impose order in the active site lid.

Reduction of FMN in the Active Site of hhIYD

The diversity of FMN-dependent catalysis in nature is based in part on its ability to function as an one and two electron acceptor and donor.[38–41] For example, reduction of nitroaromatic compounds by enzymes in the nitro-FMN reductase superfamily is promoted by stabilizing a two electron pathway and destabilizing alternative one electron pathways.[42–44] Conversely, deiodination of I-Tyr is promoted by stabilizing an one electron process at the expense of competing two electron processes.[11,44] Previous studies on human IYD demonstrated that the one electron reduced FMN semiquinone (FMN_{sq}) accumulated in the presence of either a halotyrosine substrate (I-Tyr) or its inert analogue fluorotyrosine (F-Tyr).[11] The ability of hhIYD to support a similar response to F-Tyr was confirmed by anaerobic reduction under standard conditions using xanthine/xanthine oxidase.[23,24] Most importantly, this analysis was also repeated in the presence of 2IP to learn the effect of base stacking on the stability of FMN_{sq}.

In the absence of an active site ligand, the FMN_{ox} of hhIYD (λ_{max} = 446 nm and shoulder near 470 nm) was reduced to FMN_{hq} without detection of an intermediate FMN_{sq} (λ_{max} = 590 nm) (Figure S11). Next, binding of F-Tyr to hhIYD was confirmed for its use as an inert mimic of I-Tyr to induce closure of the active site lid. By measuring quenching of FMN_{ox} fluorescence in hhIYD as described above, F-Tyr was shown to bind with a K_d of 46 ± 2 μM (Figure S12). More than a 10-fold excess of F-Tyr (500 μM) was then added to hhIYD prior its reduction. Under these conditions, accumulation of the FMN_{sq} intermediate was clearly

detected by the initial increase and then decrease in A_{590} (Figure 4A) in a manner similar to that observed with human IYD.[11]

The use of 2-fluorophenol as an inert analogue of 2IP was impractical since it bound only very weakly to hhIYD (K_d = 20 ± 1 mM) (Figure S12). Instead, 2IP was studied directly for possible stabilization of the FMN_{sq} intermediate. This was possible due to the very low efficiency of 2IP turnover. From its k_{cat} value, less than one equivalent could be dehalogenated in the time necessary for the redox titration. Consequently, 2IP (800 μM) was added to hhIYD in greater than a 10-fold excess above its K_d value (Table 1) prior to initiating reduction. During reduction, 2IP did not detectably promote an accumulation of the FMN_{sq} intermediate in contrast to the effect of F-Tyr (Figure 4B). This inability of 2IP to stabilize FMN_{sq} to a detectable extent is also consistent with its very slow turnover.

DISCUSSION

The simple halophenol 2IP binds to the active site of hhIYD in a manner equivalent to the halophenol component of the substrate I-Tyr. Crystallographic analysis reveals that both ligands stack on the isoalloxazine ring of FMN, and the hhIYD structures are mostly superposable with the corresponding structures of human and mouse IYD. In addition, the aryl-I bond is positioned over the C4a-N5 bond of FMN, a highly active region participating in redox catalysis.[41] Association between 2IP and hhIYD is likely stabilized by hydrophobic and van der Waals interactions, π-stacking with FMN, and hydrogen bonding between the phenolate form of this ligand, the peptide backbone and the 2′-HO group of the ribityl portion of FMN. These same interactions are common to all substrates and active site ligands of IYD.[10,11] However, 2IP binds only very weakly to human IYD. The differences in affinity between human IYD and hhIYD might arise from the relative dynamics and pre-organization of their active sites in the absence of ligand. Although both enzymes exhibit disorder in the helical region of the active site lid (hhIYD residues 95–112) in the absence of substrate, the adjacent loop (hhIYD residues 133–145) is ordered in hhIYD (Figure S9) and may enhance the population of conformers that readily accommodate the halophenol ligand. This affinity may be beneficial for the physiological function of IYD in bacteria but would be disadvantageous for mammalian IYD which must carefully distinguish between its halotyrosine substrate and other halophenol derivatives that are created by thyroid hormone metabolism.

Binding and orientation of the iodophenol component in the active site of IYD is not sufficient to drive reductive dehalogenation. This is best demonstrated by the derivative 2IPCN that binds to hhIYD with a greater affinity than I-Tyr but does not participate in catalysis (Table 1). This characteristic is not shared by other enzymes in the same structural superfamily for which reactivity is often dictated by proximity. For example, NADH directly reduces FMN bound to nitroreductase NfsB (*E. coli*) and nicotinic acid has been observed to stack directly over the isoalloxazine ring of FMN in a co-crystal with nitroreductase NfsB (*E. coli*.).[13] Similar orientations of substrates stacking over the isoalloxazine ring have been observed in co-crystals of NFsB with dinitrobenzamide prodrugs and dicoumarol[45] and co-crystals of flavin reductase (*Vibrio fischeri*) with dicoumarol.[46] Even the regiospecificity of dinitroaromatic reduction can be manipulated by altering the orientation of the two nitro

groups with respect to their stacking over the FMN of NfsB.[47] In contrast, no redox exchange occurs between the electron acceptor iodophenol and the electron donor FMN_{hq} even when stacked together in the active site of IYD.

Substrate specificity for both mammalian and *H. hydrossis* IYD is consequently a function of selective activation of the catalytic chemistry required for dehalogenation. The redox properties of flavin are often modulated by π-stacking as measured previously in both models systems[48] and numerous flavoproteins.[16,49–51] Such π-interactions are not sufficient for IYD catalysis since both active (I-Tyr) and inactive (2IP) compounds demonstrate similar abilities to stack above the active site FMN (Figure 3). Instead, the major determinant for dehalogenation is likely based on the extent to which FMN can participate in single electron transfer.[11,44] Major activity classes within the nitro-FMN reductase superfamily can be distinguished by their alternative ability to promote one and two electron processes of FMN. An obligate two electron transfer is catalyzed by the nitroreductases in this superfamily and competing one electron chemistry to form FMN_{sq} is actively suppressed.[42,43] This may in part be related to the hydrogen bonding between the amide backbone and FMN N5. Human IYD promotes FMN_{sq} formation once substrate binds to the active site and induces a conformational shift allowing Thr239 to approach for hydrogen bonding between its side chain hydroxyl group and FMN N5.[11] This type of hydrogen bonding is often associated with activation of one electron pathways but it can also influence hydride transfer as well.[52–54] For human IYD, the interactions between the side-chain of Thr239 and FMN N5 have a profound effect on catalysis and act as a switch between one and two electron processes.[44]

Crystal structures of hhIYD in the absence and presence of I-Tyr illustrate a substrate-dependent closure of the active site lid similar to that characterized previously for human IYD (Figure 2).[11] However, a key hydrogen bond induced by closure of the active site lid in mammalian IYD differs from that observed for hhIYD. In human IYD bound with I-Tyr, Thr239 is within hydrogen bonding range of FMN N5 (3.1Å) but is 4.9 Å away in the absence of I-Tyr (Figure 5A). In hhIYD, the equivalent residue, Thr173, does not move into close proximity with the FMN N5 upon binding of I-Tyr (Figure 5B). Instead, Thr173 exists in multiple conformations and its oxygen remains at an intermediate distance from the N5 position of FMN (3.6–4.0 Å). This intermediate distance is also observed between Thr173 and FMN N5 in the structure of hhIYD bound with 2IP (Figure 5C). The limited motion of the loop containing Thr173 in hhIYD may result from constraints conferred by Pro176 that is replaced by Asn 242 in human IYD (Figure 5). Still, Thr173 is key to single electron transfer by IYD. A mutation of T173A in hhIYD suppresses FMN_{sq} formation and I-Tyr dehalogenation while concurrently promoting nitroaromatic reduction.[44] Additionally, binding of F-Tyr to hhIYD clearly affects its ability to stabilize FMN_{sq} during reductive titration (Figure 4). Similar stabilization is not evident after association of hhIYD with 2IP. Thus, the zwitterion dominants catalytic activation of IYD and suggests that halotyrosines are the likely substrates for bacterial as well as mammalian IYD. The details of substrate dependent activation of hhIYD and the expected hydrogen bonding between Thr173 and FMN N5 may be clarified after a crystal structure of the reduced FMN_{hq} form of IYD•F-Tyr can determined.

CONCLUSION

The specificity of human IYD is easily rationalized by its physiological role to salvage iodide from I-Tyr while avoiding dehalogenation of other iodophenol-containing materials associated with thyroid hormone biosynthesis and regulation. The iodophenol component neither binds to human IYD nor participates in catalytic turnover efficiently. The constraints for the bacteria homolog hhIYD were not anticipated since its natural substrates and metabolic function have yet to be established. Although hhIYD does not discriminate as well as human IYD for binding halotyrosine versus halophenol derivatives, their catalytic selectivity remains similar. Both require the zwitterion of halotyrosine to stabilize the formation of FMN_{sq} directly or indirectly and facilitate the single electron transfer process that appears necessary for reductive dehalogenation.[44] The basal level of iodophenol deiodination is very low and not likely relevant in nature. Thus, active site stacking of substrate and FMN is not sufficient for reductive deiodination despite the close proximity of the reactants. Since iodide is not a known requirement for bacteria, hhIYD has the potential to consume halotyrosines if present in their environment. hhIYD may also contribute to secondary metabolism in analogy to a recently discovered reductive debrominase that is required for the biosynthesis of a marine natural product.[55]

Supplementary Material

Refer to Web version on PubMed Central for supplementary material.

Acknowledgments

Funding

This work was supported in part by the National Institutes of Health (NIH) grant AI119540. Use of the Stanford Synchrotron Radiation Lightsource (SLAC) at the National Accelerator Laboratory is supported by the U.S. Department of Energy, Office of Basic Energy Sciences under Contract No. DE-AC02-76SF00515. The SSRL Structural Molecular Biology Program is supported by the DOE Office of Biological and Environmental Research, and by the National Institute of General Medical Sciences (including P41GM103393).

We thank Jimin Hu and Jennifer Buss for providing plasmids encoding the human IYD and hhIYD genes

ABBREVIATIONS

4A2IP	4-amino-2-iodophenol
I_2-Tyr	3,5-diiodo-L-tyrosine
FMN	flavin mononucleotide
FMN_{hq}	reduced FMN hydroquinone
FMN_{ox}	oxidized FMN
FMN_{sq}	one-electron reduced FMN semiquinone
F-Tyr	3-fluoro-L-tyrosine
2FP	2-fluorophenol

2IP	2-iodophenol
2IPCN	4-cyano-2-iodophenol
2IPCOOH	4-hydroxy-3-iodobenzoic acid
I-Tyr	3-iodo-L-tyrosine
IYD	iodotyrosine deiodinase
hhIYD	IYD from bacterium *Haliscomenobacter hydrossis* (DSM 1100)
RMSD	root mean squared deviation
TCEP	tris(2-carboxyethyl)phosphine hydrochloride

References

1. Roche J, Michel O, Michel R, Gorbman A, Lissitzky S. Sur la Deshalogénation Enzymatique des Iodotyrosines par le Corps Thyroïde et sur son Rôle Physiologique. II. Biochim Biophys Acta. 1953; 12:570–576. [PubMed: 13140266]
2. Cavalieri RR. Iodine Metabolism and Thyroid Physiology: Current Concepts. Thyroid. 1977; 7:177–181.
3. Moreno JC, Klootwijk W, van Toor H, Pinto G, D'Alessandro M, Lèger A, Goudie D, Polak M, Grüters A, Visser TJ. Mutations in the Iodotryosine Deiodinase Gene and Hypothyroidism. N Engl J Med. 2008; 358:1811–1818. [PubMed: 18434651]
4. Delange F. Iodine Deficiency in Europe and its Consequences: an Update. Eur J N Med Mol I. 2002; 29:S404–S416.
5. Zimmermann MB. Iodine Deficiency. Endocr Rev. 2009; 30:376–408. [PubMed: 19460960]
6. Rokita, SE. Flavoprotein Dehalogenases. In: Hille, R.Miller, SM., Palfey, B., editors. Handbook of Flavoproteins. Vol. 1. DeGruyter; Berlin: 2013. p. 337-350.
7. McTamney PM, Rokita SE. A Mammalian Reductive Deiodinase has Broad Power to Dehalogenate Chlorinated and Brominated Substrates. J Am Chem Soc. 2009; 131:14212–14213. [PubMed: 19777994]
8. Bobyk KD, Ballou DP, Rokita SE. Pre-Steady-State Characterization of Iodotyrosine Deiodinase from Human Thyroid. Biochemistry. 2015; 54:4487–4494. [PubMed: 26151430]
9. Solis-S JC, Villalobos P, Valverde-R C. Comparative Kinetic Characterization of Rat Thyroid Iodotyrosine Dehalogenase and Iodothyronine Deiodinase Type 1. J Endocrinol. 2004; 181:385–392. [PubMed: 15171686]
10. Thomas SR, McTamney PM, Adler JM, LaRonde-LeBlanc N, Rokita SE. Crystal Structure of Iodotyrosine Deiodinase, a Novel Flavoprotein Responsible for Iodide Salvage in Thyroid Glands. J Biol Chem. 2009; 284:19659–19667. [PubMed: 19436071]
11. Hu J, Chuenchor W, Rokita SE. A Switch Between One- and Two-Electron Chemistry of the Human Flavoprotein Iodotyrosine Deiodinase is Controlled by Substrate. J Biol Chem. 2015; 290:590–600. [PubMed: 25395621]
12. Shimizu R, Yamaguchi M, Uramaru N, Kuroki H, Ohta S, Kitamura S, Sugihara K. Structure–Activity Relationships of 44 Halogenated Compounds for Iodotyrosine Deiodinase-Inhibitory Activity. Toxicology. 2013; 314:22–29. [PubMed: 24012475]
13. Lovering AL, Hyde EI, Searle PF, White SA. The Structure of *Escherichia coli* Nitroreductase Complexes with Nicontinic Acid: Three Crystal Forms at 1.7 Å, 1.8 Å and 2.4 Å Resolution. J Mol Biol. 2001; 309:203–213. [PubMed: 11491290]
14. Johansson E, Parkinson GN, Denney EJ, Neidle S. Studies on the Nitroreductase Prodrug-Activating System. Crystal Structures of Complexes with the Inhibitor Dicoumarol and

Nitrobenzamide Prodrugs and of the Enzyme Active Form. J Med Chem. 2003; 46:4009–4020. [PubMed: 12954054]

15. Wang CJ, Hagemeier C, Rahman N, Lowe E, Noble M, Coughtrie M, Sim E, Westwood I. Molecular Cloning, Characterization and Ligand-Bound Structure of an Azoreductase from *Pseudomonas aruginosa*. J Mol Biol. 2007; 373:1213–1228. [PubMed: 17904577]
16. Lostao A, Gómez-Moreno C, Mayhew SG, Sancho J. Differential Stabilization of the Three FMN Redox Forms by Tyrosine 94 and Tryptophan 57 in Flavodoxin from *Anabeaena* and its Influence on the Redox Potentials. Biochemistry. 1997; 36:14334–14344. [PubMed: 9398151]
17. Edgar KJ, Falling SN. An Efficient and Selective Method for the Preparation of Iodophenols. J Org Chem. 55:5287–5291.
18. Phatarphekar A, Buss JM, Rokita SE. Iodotyrosine Deiodinase: a Unique Flavoprotein Present in Organisms of Diverse Phyla. Mol BioSyst. 2014; 10:86–92. [PubMed: 24153409]
19. Pace CN, Vajdos F, Fee L, Grimsley G, Gray T. How to Measure and Predict the Molar Absorption Coefficient of a Protein. Protein Sci. 1995; 4:2411–2423. [PubMed: 8563639]
20. Koziol J. Fluorometric Analyses of Riboflavin and its Coenzymes. Methods Enzymol. 1971; 18:235–285.
21. McTamney PM, Rokita SE. A Mammalian Reductive Deiodinase has broad Power to Dehalogenate Chlorinated and Brominated Substrates. J Am Chem Soc. 2009; 131:14212–14213. [PubMed: 19777994]
22. Phatarphekar A, Rokita SE. Functional Analysis of Iodotyrosine Deiodinase from *Drosophila melanogaster*. Protein Sci. 2016; 25:2187–2195. [PubMed: 27643701]
23. Massey, V. A Simple Method for the Determination of Redox Potentials. In: Curti, B.Ronchi, S., Zanetti, G., editors. Flavins Flavoproteins Proc Int Symp. Gruyter & Co.; Berlin: 1991. p. 59-66.
24. van den Heuvel RHH, Fraaije MW, Van Berkel WJH. Redox Properties of Vanillyl-Alcohol Oxidase. Methods Enzymol. 2002; 353:177–186. [PubMed: 12078493]
25. Kabsch W. Automatic Processing of Rotation Diffraction Data from Crystals of Initially Unknown Symmetry and Cell Constants. J Appl Cryst. 1993; 26:795–800.
26. Otwinowski, Z., Minor, W. Methods in Enzymology. Academic Press; 1997. [20] Processing of X-ray Diffraction Data Collected in Oscillation Mode; p. 307-326.
27. McCoy AJ, Grosse-Kunstleve RW, Adams PD, Winn MD, Storonia LC, Reada RJ. Phaser Crystallographic Software. J Appl Cryst. 2007; 40:658–674. [PubMed: 19461840]
28. Emsley P, Cowtan K. Coot: Model-Building Tools for Molecular Graphics. Acta Cryst. 2004; 60:2126–2132.
29. Adams PD, Afonine PV, Bunkóczi G, Chen VB, Davis IW, Echols N, Headd JJ, Hung L-W, Kapral GJ, Grosse-Kunstleve RW, McCoy AJ, Moriarty NW, Oeffner R, Read RJ, Richardson DC, Richardson JS, Terwilliger TC, Zwart PH. PHENIX: a Comprehensive Python-Based System for Macromolecular Structure Solution. Acta Cryst. 2010; 66:213–221.
30. Buss JM, McTamney PM, Rokita SE. Expression of a Soluble Form of Iodotyrosine Deiodinase for Active Site Characterization by Engineering the Native Membrane Protein from *Mus musculus*. Protein Sci. 2012; 21:351–361. [PubMed: 22238141]
31. Gasteiger, E., Hoogland, C., Gattiker, A., Duvaud, S., Wilkins, MR., Appel, RD., Bairoch, A. Protein Identification and Analysis Tools on the ExPASy Server. In: Walker, JM., editor. The Proteomics Protocols Handbook. Humana Press; 2005. p. 571-607.
32. Heyland A, Hodin J, Reitzel AM. Hormone Signaling in Evolution and Development: a Non-model System Approach. BioEssays. 2005; 27:64–75. [PubMed: 15612033]
33. Miller AEM, Heyland A. Iodine Accumulation in Sea Urchin Larvae is Dependent on Peroxide. J Exp Biol. 2013; 216:915–926. [PubMed: 23155081]
34. Rokita SE, Adler JM, McTamney PM, Watson JA Jr. Efficient Use and Recycling of the Micronutrient Iodide in Mammals. Biochimie. 2010; 92:1227–1235. [PubMed: 20167242]
35. Friedman JE, Watson JA Jr, Lam DWH, Rokita SE. Iodotyrosine Deiodinase is the First Mammalian Member of the NADH Oxidase/Flavin Reductase Superfamily. J Biol Chem. 2006; 281:2812–2819. [PubMed: 16316988]

36. Li Y, Reilly PJ, Ford C. Effect of Introducing Proline Residues on the Stability of *Aspergillus awamori*. Protein Eng. 1997; 10:1199–1204. [PubMed: 9488144]
37. Gilday LC, Robinson SW, Barendt TA, Langton MJ, Mullaney BR, Beer PD. Halogen Bonding in Supramolecular Chemistry. Chem Rev. 2015; 115:7118–7195. [PubMed: 26165273]
38. Massey V. The Chemical and Biological Versatility of Riboflavin. Biochem Soc Trans. 2000; 28:283–296. [PubMed: 10961912]
39. Fraaije MW, Mattevi A. Flavoenzymes: Diverse Catalysts with Recurrent Features. Trends Biochem Sci. 2000; 25:126–132. [PubMed: 10694883]
40. Mansoorabadi SO, Thibodeaux CJ, Liu H-w. The Diverse Roles of Flavin Coenyzmes—Nature's Most Versatile Thespians. J Org Chem. 2007; 72:6329–6342. [PubMed: 17580897]
41. Fagan, RL., Palfey, BA. Flavin-Dependent Enzymes. In: Begley, TP., editor. Ch. 3 in Comprehensive Natural Products II. Elsevier; Oxford: 2010. p. 37-114.
42. Haynes CA, Koder RL, Miller AF, Rodgers DW. Structures of Nitroreductase in Three States. J Biol Chem. 2002; 277:11513–11520. [PubMed: 11805110]
43. Koder RL, Haynes CA, Rodgers ME, Rodgers DW, Miller AF. Flavin Thermodynamics Explain the Oxygen Insensitivity of Enteric Nitroreductase. Biochemistry. 2002; 41:14197–14205. [PubMed: 12450383]
44. Mukherjee A, Rokita SE. Single Amino Acid Switch Between a Flavin-Dependent Dehalogenase and Nitroreductase. J Am Chem Soc. 2016; 137:15342–15345.
45. Johansson E, Parkinson GN, Denny WA, Neidle S. Studies on the Nitroreductase Prodrug-Activating System. Crystal Structures of Complexes with the Inhibitor Dicoumarol and Dinitrobenzamide Prodrugs and of the Enzyme Active Form. J Med Chem. 2003; 46:4009–4020. [PubMed: 12954054]
46. Koike H, Sasaki H, Kobori T, Zenno S, Saigo K, Murphy MEP, Adman ET, Tanokura M. 1.8 Å Crystal Structure of the Major NAD(P)H:FMN Oxidoreductase of a Bioluminescent Bacterium, *Vibrio fischeri*: Overall Structure, Cofactor and Substrate-Analog Binding, and Comparison with Related Flavoproteins. J Mol Biol. 1998; 280:259–273. [PubMed: 9654450]
47. Bai J, Zhou Y, Chen Q, Yang Q, Yang J. Altering the Regioselectivity of a Nitroreductase in the Synthesis of Arylhydroxylamines by Structure-Based Engineering. ChemBioChem. 2015; 16:1219–1225. [PubMed: 25917861]
48. Breinlinger EC, Rotello VM. Model Systems for Flavoenzyme Activity. Modulation of Flavin Redox Potentials through π-Stacking Interactions. J Am Chem Soc. 1997; 119:1165–1166.
49. Swenson RP, Krey GD. Site-Directed Mutagenesis of Tyrosine-98 in the Flavodoxin from *Desulfovibrio vulgaris* (Hildenborough): Regulation of Oxidation- Reduction Properties of the Bound FMN Cofactor by Aromatic, Solvent and Electrostatic Interactions. Biochemistry. 1994; 33:8505–8514. [PubMed: 8031784]
50. Pellett JD, Becker DF, Saenger AK, Fuchs JA, Stankovich MT. Role of Aromatic Stacking Interactions in the Modulation of the Two-Electron Reduction Potentials of Flavin and Substrate/Product in *Megasphaera elsdenii* Short-Chain Acyl- Coenzyme a Dehydrogenase. Biochemistry. 2001; 40:7720–7728. [PubMed: 11412126]
51. Seo D, Naito H, Nishimura E, Sakurai T. Replacement of Tyr50 Stacked on the si-Face of the Isoalloxazine Ring of the Flavin Adenine Dinucleotide Prosthetic Group Modulates *Bacillus subtilis* Ferredoxin-$NADP^+$ Oxidoreductase Activity Toward NADPH. Photosyn Res. 2015; 125:321–328. [PubMed: 25698107]
52. Taga ME, Larsen NA, Howard-Jones AR, Walsh CT, Walker GC. BluB Cannibalizes Flavin to Form the Lower Ligand of Vitamin B_{12}. Nature. 2007; 446:449–453. [PubMed: 17377583]
53. Pitsawong W, Sucharitakul J, Prongjit M, Tan TC, Spadiut O, Haltrich D, Divne C, Chaiyen P. A Conserved Active-Site Threonine is Important for Both Sugar and Flavin Oxidations of Pyranose 2-Oxidase. J Biol Chem. 2010; 285:9697–9705. [PubMed: 20089849]
54. Yuan H, Gadda G. Importance of a Serine Proximal to the C(4a) and N(5) Flavin Atoms for Hydride Transfer in Choline Oxidase. Biochemistry. 2011; 50:770–779. [PubMed: 21174412]
55. El Gamal A, Agarwal V, Rahman I, Moore BS. Enzymatic Reductive Dehalogenation Controls Biosynthesis of Marine Bacterial Pyrroles. J Am Chem Soc. 2016; 138:13167–13179. [PubMed: 27676265]

56. Penhoat M. Scope and Limitations of a ^{1}H NMR Method for the Prediction of Substituted Phenols pKa Values in Water, CH_3CN, DMF, DMSO and i-PrOH. Tetrahedron Lett. 2013; 54:2571–2574.

57. Stradins J, Hasanli B. Anodic Voltammetry of Phenol and Benzenethiol Derivatives: Part 1 Influence of pH on Electro-Oxidation Potentials of Substituted Phenols and Evaluation of pK_a from Anodic Voltammetry Data. J Electroanal Chem. 1993; 353:57–69.

58. Das TN. Redox Chemistry of 3-Iodotyrosine in Aqueous Medium. J Phys Chem A. 1998; 102:426–433.

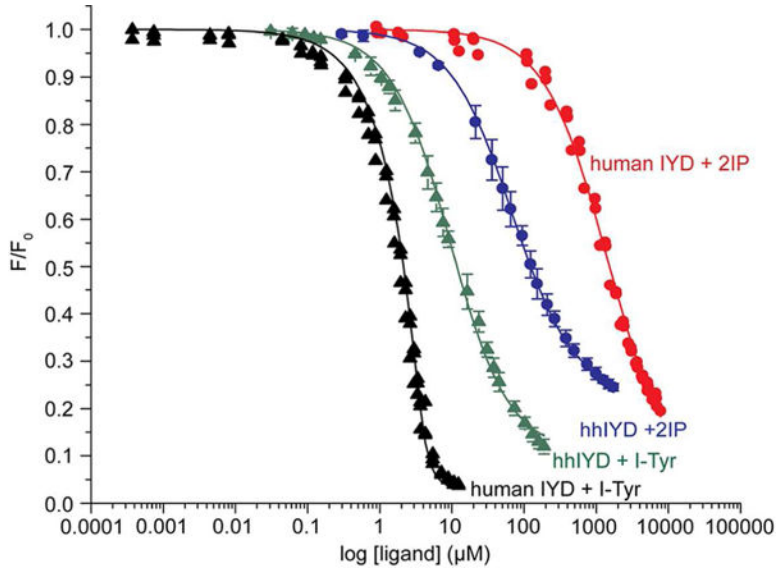

Figure 1.

Quenching of FMN_{ox} fluorescence as a monitor for substrate binding to IYD. Human IYD (4.3 μM and 200 mM KCl) and hhIYD (2.5 μM) in 100 mM potassium phosphate pH 7.4 were stirred at 25 °C for 30 min prior to addition of the indicated ligand. The K_d values were determined from the best fit to quenching of FMN_{ox} fluorescence using λ_{ex} and λ_{em} of 450 nm and 523 nm, respectively, as described previously.[11]

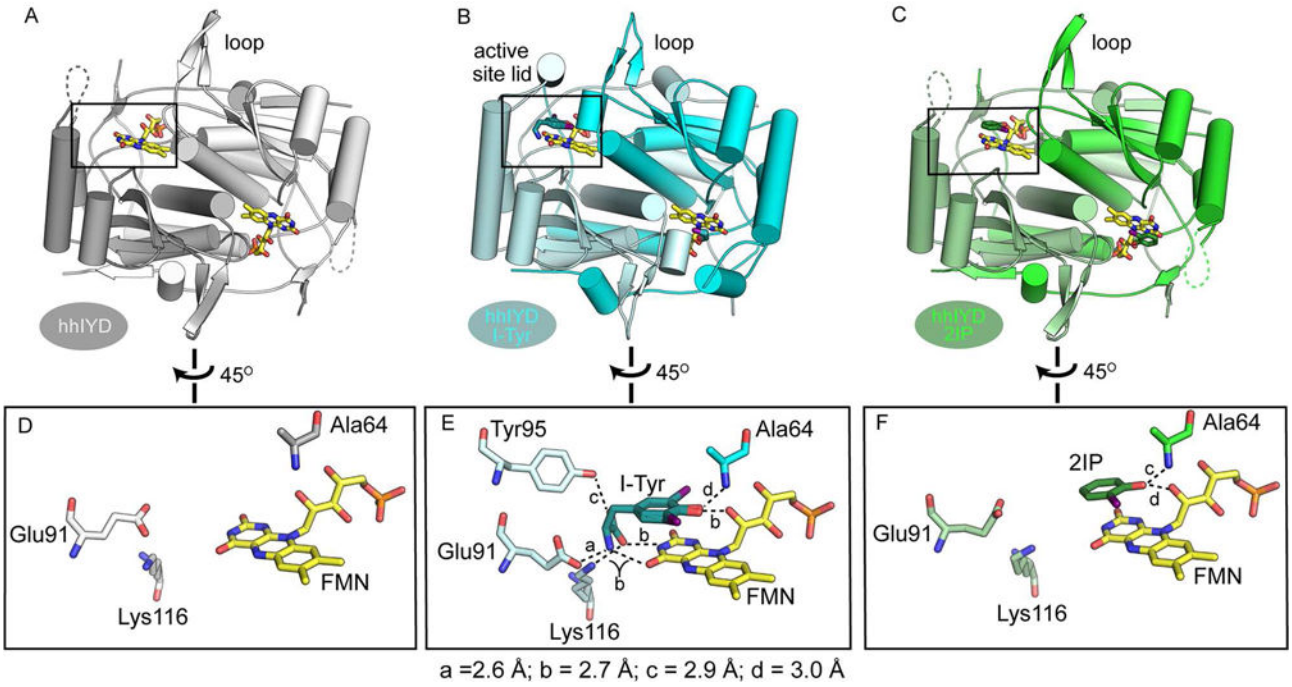

Figure 2.

Structures of hhIYD and the environment surrounding its bound FMN. Cartoon representation of the structure of the homodimers of (A) hhIYD (grey), (B) hhIYD·I-Tyr (cyan) and (C) hhIYD·2IP (green). Individual polypeptides are indicated by their different shades of color and disordered regions are indicated by the dashed lines. The active site environment surrounding FMN (carbon atoms in yellow) is illustrated for (D) hhIYD, (E) hhIYD·I-Tyr and (F) hhIYD·2IP.

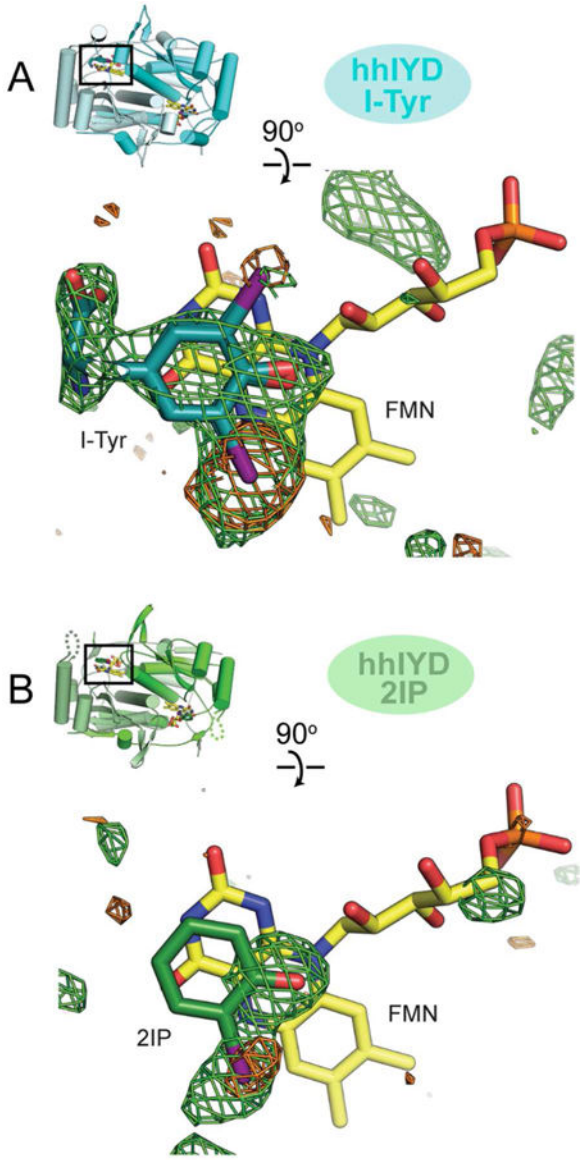

Figure 3.

Orientation of the substrate-FMN_{ox} complex in the active site of hhIYD. Bound FMN_{ox} is indicated by its yellow carbon atoms. (A) Two configurations of I-Tyr (carbons in cyan) are evident from the two positions of the aryl iodide. (B) Only a single configuration of 2IP (carbons in green) was detected. The unbiased F_o-F_c difference maps contoured at +3σ are shown by the green mesh. Anomalous difference maps contoured at +3σ are shown by the orange mesh.

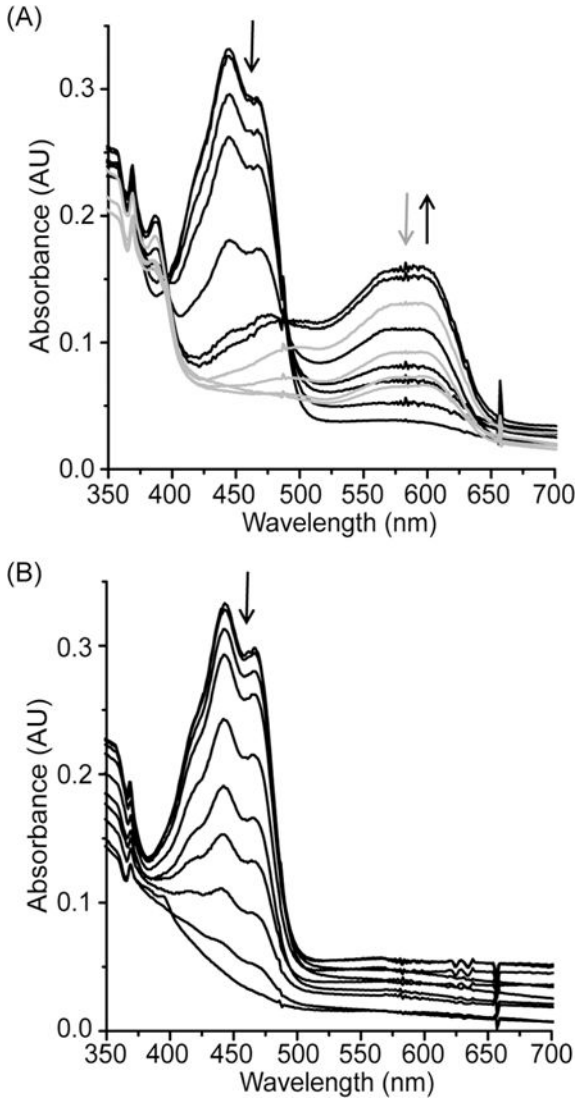

Figure 4.

Anaerobic reduction of FMN bound to hhIYD by xanthine and xanthine oxidase as monitored by absorbance spectroscopy. Sample spectra of hhIYD (20 μM) over 40 min indicate the reduction of FMN by loss of absorbance (~ 450 nm) in the presence of (A) F-Tyr (500 μM) and (B) 2IP (800 μM). Absorbance (~590 nm) increases (black) and then decreases (grey) only during reduction in (A).

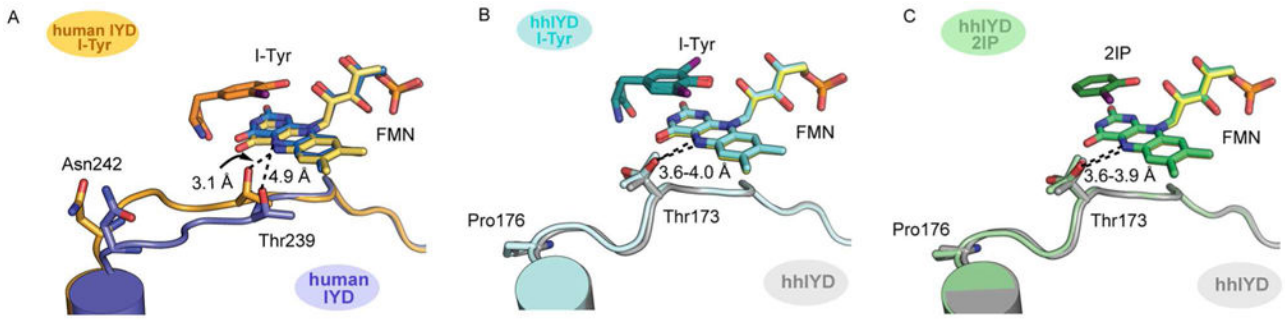

Figure 5.

Conformational dependence for hydrogen bonding between a Thr and the N5 position of FMN_{ox}. (A) Cartoon representation of the superposition of human IYD in the absence (blue) and presence of I-Tyr (orange). (B) Equivalent superposition of hhIYD in the absence (grey) and presence of I-Tyr (cyan). (C) Equivalent superposition of hhIYD in the absence (grey) and presence of 2IP (green).

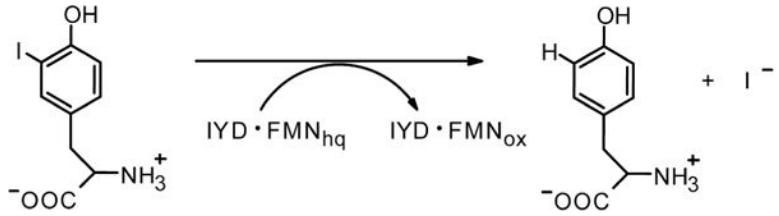

Scheme 1.

Iodotyrosine deiodinase (IYD) reduces I-Tyr as it oxidizes its bound FMN_{hq}.

Table 1

Binding affinity and kinetic parameters for human IYD and hhIYD.

IYD	Substrate	R	pK_a (phenol)	K_d (μM)[c]	k_{cat} (× 10^{-2} s^{-1})[d]	K_m (mM)[d]	k_{cat}/K_m (M^{-1} s^{-1})
Human	I-Tyr	–	8.4,[a] 8.3[b]	0.09 ± 0.02	10.2 ± 0.4	0.0073 ± 0.0008	(1.4 ± 2) × 10^4
	2IP	H	8.4,[a] 8.5[b]	1,410 ± 70	0.40 ± 0.02	4.1 ± 0.4	1.0 ± 0.1
hhIYD	I-Tyr	–	8.4,[a] 8.3[b]	8.2 ± 0.5	27 ± 2	0.0012 ± 0.0002	(23 ± 4) × 10^4
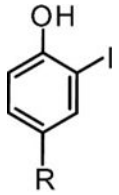	2IP	H	8.4,[a] 8.5[b]	67 ± 2	0.29 ± 0.03	4.1 ± 0.8	0.7 ± 0.2
	4A2IP	NH2	9.3[a]	96 ± 3	–	–	4.1 ± *0.3*[f]
	2IPCOOH	COO^-	8.6[a]	24.1 ± 0.7	0.31 ± 0.01	7.1 ± 0.6	0.44 ± 0.04
	2IPCN	CN	6.7[a]	1.44 ± 0.05	< 2.1 × 10^{-3}[e]	–	–

[a] pK_a values of the phenolic protons were calculated with the ACE and JChem acidity and basicity calculator (https://epoch.uky.edu/ace/public/pKa.jsp).

[b] pK_a values were also determined experimentally as published previously[56–58]

[c] Determined from data of Figures 1 and S4.

[d] Determined from data of Figure S7.

[e] Estimated from the detection threshold of 4-cyanophenol (Figure S6B).

[f] Estimated from Lineweaver–Burk analysis. Errors derive from least squares fitting.

Table 2

Data collection and refinement statistics

Protein	hhIYD	hhIYD•I-Tyr	hhIYD•2IP
Ligands	FMN	FMN and I-Tyr	FMN and 2IP
Protein Data Bank code	5KO7	5KO8	5KRD
Data collection			
Space group	P 2_1 2_1 2	P 6_2 2 2	P 6_4 2 2
Unit cell parameters			
a, b, c (Å)	92.18, 110.88, 43.29	152.72, 152.72, 87.20	154.70, 154.70, 88.88
α, *β*, γ (°)	90, 90, 90	90, 90, 120	90, 90, 120
Resolution (Å)[a]	36.96–2.25 (2.32–2.25)	38.18–2.15 (2.22–2.15)	20.00–2.10 (2.17–2.10)
Wavelength (Å)	1.127	0.980	0.980
No. of unique reflections[a]	21,635 (1,685)	33,077 (2,795)	36,523 (3,607)
No. of observed reflections	149,492	647,766	267,636
Completeness (%)[a]	98.9 (88.4)	99.9 (100)	98.8 (99.5)
Redundancy[a]	6.9 (5.1)	19.6 (20.4)	7.3 (7.2)
R_{sym} (%)[a,b]	7.5 (145)	14.7 (375)	10.7 (100)
$R_{p.i.m}$ (%)[a,c]	3.1 (69.4)	3.4 (84.0)	5.7 (100)
$I/\sigma I$[a]	15.2 (1.1)	16.8 (1.1)	15.2 (1.0)
Refinement			
Resolution used inrefinement (Å)	35.4–2.3	38.2–2.2	20.0–2.1
R_{work} (%)/R_{free} (%)[d]	21.6/25.4	19.1/23.2	17.7/22.1
No. of atoms			
Protein	6,336	6,925	6,401
Heteroatoms	100 (FMN)	174 (FMN and I-Tyr)	116 (FMN and 2IP)
Solvent	62	128	126
Mean *B*-factor (Å^2)			
Protein	71.25	62.44	60.16
Waters	53.47	50.96	56.18
FMN	56.22	44.21	45.74
I-Tyr	–	62.57	–
2IP	–	–	65.46
RMSD from ideality			
Bond lengths (Å)	0.003	0.005	0.014
Bond angles (°)	0.707	0.842	1.386
Ramachandran analysis			
Favored (%)	99.49	98.60	99.49
Allowed (%)	0.51	1.40	0.51

Outliers	0	0	0

[a] The values in parentheses are for the highest resolution shell.

[b] R_{sym} =ΣhklΣi |Ii −<I>|/ΣhklΣi Ii, where Ii is the intensity of an individual reflection and <I> is the mean intensity obtained from multiple observations of symmetry related reflections.

[c] $R_{p.i.m}$ =Σhk1√((1/(n-1)) Σi |Ii − <I>|/ΣhklΣi Ii, where Ii is the intensity of an individual reflection and <I> is the mean intensity obtained from multiple observations of symmetry related reflections.

[d] R_{work} = Σhkl (|F_{obs}| − | F_{calc} |)/Ehkl | F_{obs} | where F_{obs} is an observed amplitude and F_{calc} a calculated amplitude; R_{free} is the same statistic calculated over a subset of the data that has not been used for refinement.